Evaluation of the magnetic moment of ^{213}Ra

Surya N. Panigrahy, R. W. Dougherty, S. Ahmad, K. C. Mishra,* and T. P. Das
Department of Physics, State University of New York at Albany, Albany, New York 12222

J. Andriessen
Technische Natuurkunde, Technische Hogeschool Delft, 2628 CJ Delft, The Netherlands

R. Neugart, E. W. Otten, and K. Wendt
Institut für Physik, der Universität Mainz, 6500 Mainz, Federal Republic of Germany
(Received 18 January 1990; revised manuscript received 16 July 1990)

The hyperfine field at the nucleus of singly ionized radium has been investigated using the relativistic linked-cluster many-body-perturbation-theory procedure, including the effects of distributed charge and magnetization over the nucleus. The total hyperfine field of 1239 T, when combined with the experimentally observed hyperfine constant for $^{213}Ra^+$, yields a nuclear moment of $0.607(12)\mu_N$, in excellent agreement with the experimentally observed moment of $0.6133(18)\mu_N$ from Zeeman measurements. Our investigation leads to exchange core-polarization and correlation contributions of 14% and 13%, respectively, of the direct contribution of the 7*s* valence electron, these ratios being smaller than the corresponding ratios for the isoelectronic atom francium, in keeping with the expected trends for other isoelectronic alkaline-earth-metal ions and alkali-metal atoms. Comparison is made with the results of other calculations of the nuclear moment of ^{213}Ra. Possible reasons for the success of the semiempirical Goudsmit-Fermi-Segre formula in predicting the hyperfine field in this ion and related systems will be discussed.

I. INTRODUCTION

The magnetic moment of the ^{213}Ra nucleus has recently been measured[1] with great accuracy by three of the authors of the present paper (Neugart, Otten, and Wendt) in collaboration with several others by observing the Larmor precession of the nucleus in an external magnetic field using collinear-laser-beam spectroscopy. Since the magnetic hyperfine constants of several of the radium nuclei in Ra^+ had already been measured[2] by the same group, one can also use the theoretically obtained magnetic field at the nucleus of the Ra^+ ion to extract the nuclear moments of the nuclei including ^{213}Ra. The comparison between the nuclear moment of ^{213}Ra obtained by this method with that obtained through direct experimental measurement[1] by the Zeeman effect technique thus provides a stringent test of the theory, which has been possible in the past for only one other comparably heavy atom, namely, francium.[3,4] In the present work we have used the relativistic linked-cluster many-body perturbation theory[5] (RLCMBPT), previously applied successfully to a number of other atomic systems,[5–7] to calculate the hyperfine field at the nucleus of Ra^+. The magnetic moment of ^{213}Ra thus derived is shown to agree within 2% with the experimental value.[1] Comparison will be made between the results of the present calculation and earlier results[8] obtained by the present group. Additionally, there are two other calculations[9,10] reported in the literature which have used a variant of the RLCMBPT procedure adopted in the present work, calculating some or all of the vertices involved in the diagrams by a differential-equation (DE) approach. A comparison of the results of the present calculation is made with those of these earlier calculations,[9,10] continuing the process started in a recent publication[11] on the light lithiumlike systems of the second period. We believe that comparisons of this nature provide valuable insights into the potentialities of the different many-body procedures and a better understanding of the various mechanisms contributing to many-body effects in hyperfine interactions. Finally, a comparison will be made between the predictions[2] of the hyperfine field at the nucleus of Ra^+ by the Goudsmit-Fermi-Segre formula[12] and the results of the first-principles procedure adopted in this work. Possible reasons for the reasonable agreement between the two results will be discussed.

In Sec. II we present a brief summary of the RLCMBPT procedure. Section III presents the results of our investigation of the magnetic hyperfine field in Ra^+ and the nuclear magnetic moment of ^{213}Ra, along with a discussion and comparison with the results from experiment[1] and from other theoretical investigations.[8–10] Section IV discusses the conclusions from the present work.

II. PROCEDURE

The RLCMBPT procedure[5] has been used for some time to calculate various properties of a number of atomic systems,[3,6,7,13] with very satisfactory results. Because of this, the major aspects of the theory have been presented in some detail in earlier works.[3,5–7] We therefore give here only a brief summary of the theory for the sake of completeness. A number of other many-body perturbation procedures related to the RLCMBPT procedure used here have been utilized[9,10,14] in the literature for the

study of energy-related and hyperfine properties. Two of these procedures, as pointed out in the Introduction, have been applied[9,10] to Ra^+ and a detailed comparison between the results of these calculations and ours will be made in Sec. III.

The relativistic Hamiltonian for an atomic system of N interacting electrons is given by[5]

$$\mathcal{H}=\sum_{i=1}^{N}(c\boldsymbol{\alpha}_i\cdot\mathbf{p}_i+\beta_i mc^2)+\sum_{i=1}^{N}V_{\rm nuc}(r_i)+\sum_{i>j}\frac{e^2}{r_{ij}}\ . \tag{1}$$

Here the $\boldsymbol{\alpha}$ and β are the standard Dirac matrices. The term $V_{\rm nuc}(r_i)$ represents the potential energy experienced by the electron in the Coulomb field of the nucleus. As seen in earlier work[9,4] on the francium atom, the departure of the nuclear charge distribution from the point charge approximation has a very significant effect on the hyperfine interaction in heavy atoms. In our present work, as in francium, we have therefore used a uniform sphere approximation for the nucleus, distributing the total charge of ζe (ζ referring to the atomic number of the nucleus) uniformly throughout the volume of a sphere with radius $1.2A^{1/3}$ fm, A being the mass number of the nucleus. The Hamiltonian in Eq. (1) has not considered the influence of the Breit interaction or the interaction of the electron with its own radiation field. The influence of these effects has been studied[15] carefully for the total energies in a number of atomic systems. For hyperfine structure, the influence of the Breit interaction has been found to be significant[5,6,16,17] only for half-filled valence shells with non-s electrons, especially for nuclear quadrupole interactions.[16,17] It is not expected to be significant in effect in the present case where we are considering the magnetic hyperfine interaction for a system with an s valence electron. The radiative effect has been shown,[11] even for the highly ionized Bi^{80+} (lithiumlike system) with a large effective charge, to be quite small when compared to the contributions from the other mechanisms to the magnetic hyperfine interaction. It would be expected to make a negligible contribution in the singly charged Ra^+ system.

Since it is not possible to solve the Dirac equation $\mathcal{H}\Psi_0=E\Psi_0$ directly because of the $1/r_{12}$ interaction between the electrons, one has to resort to other procedures. In the RLCMBPT approach, one uses perturbation theory, taking the zero-order approximation to the Hamiltonian in Eq. (1) to be[5,18]

$$\mathcal{H}_0=\sum_{i=1}^{N}(c\boldsymbol{\alpha}_i\cdot\mathbf{p}_i+\beta_i mc^2)+\sum_{i=1}^{N}[V_{\rm nuc}(r_i)+V(r_i)] \tag{2}$$

where $V(r_i)$ is the V^{N-1} potential[6,7] defined through its matrix elements by the expression

$$\langle a|V^{N-1}|b\rangle=\sum_{m=1}^{N-1}\left\langle am\left|\frac{e^2}{r_{12}}\right|bm\right\rangle-\left\langle am\left|\frac{e^2}{r_{12}}\right|mb\right\rangle\ , \tag{3}$$

where the states m refer to occupied states of the atom. The V^{N-1} potential differs from the traditional Hartree-Fock potential (V^N) in that one state, in this case the $7s$ valence state, is excluded from the summation in Eq. (3). This potential is used because it produces more physically meaningful wave functions[18] for the excited states, with the result that perturbation expansions converge more rapidly when these states are used. We have generated bound states with principal quantum number n up to and including $n=12$ and 15 continuum states with energies corresponding to the mesh points of a 15-point Gauss-Laguerre quadrature formula.[19] In the V^{N-1} potential expression described by Eq. (3), the occupied states m are frozen in as the Hartree-Fock states in the V^N potential of Ra^+. The valence state $7s_{1/2}$ obtained by solving the V^{N-1} equations is the same as the Hartree-Fock state.[5,18] The cores are, however, somewhat different, but laddering effects connected with higher-order perturbation terms convert these V^{N-1} states into Hartree-Fock ones.[6,7] For all the occupied states, we will therefore use the Hartree-Fock states in the V^N potential for Ra^+ and excited states generated in the V^{N-1} potential for the evaluation of the perturbation diagrams occurring in the RLCMBPT procedure.

The difference between the Hamiltonians of Eq. (3) and Eq. (1) is treated as a perturbation. The many-body wave function Ψ_0 due to the Hamiltonian $\mathcal{H}$ can be written in terms of the wave function Φ_0 of the Hamiltonian $\mathcal{H}_0$ as follows:[20]

$$\Psi_0=\sum_{N=0}^{\infty}{}^{L}\left[\frac{\mathcal{H}'}{E_0-\mathcal{H}_0}\right]^N\Phi_0\ . \tag{4}$$

The function $\mathcal{H}'=\mathcal{H}-\mathcal{H}_0$ is the perturbation Hamiltonian.

The expectation value of a given operator $\mathcal{O}$ in the fully interacting system can be written in terms of the Φ_0 function as[21]

$$\langle\Psi_0|\mathcal{O}|\Psi_0\rangle=\sum_{N=0}^{\infty}\sum_{M=0}^{\infty}{}^{L}\left\langle\Phi_0\left|\left[\frac{\mathcal{H}'}{E_0-\mathcal{H}_0}\right]^N\mathcal{O}\left[\frac{\mathcal{H}'}{E_0-\mathcal{H}_0}\right]^M\right|\Phi_0\right\rangle\ . \tag{5}$$

Since we wish to calculate the hyperfine field at the nucleus of the ion, we take the operator $\mathcal{O}$ to be the relativistic hyperfine interaction operator[18]

$$\mathcal{O}=ec\sum_i\boldsymbol{\alpha}\cdot\frac{\boldsymbol{\mu}\times\mathbf{r}_i}{r_i^3} \tag{6}$$

where $\boldsymbol{\mu}$ is the nuclear moment. The hyperfine field is thus given by[7]

$$H(0)=\frac{\langle\Psi_0|\mathcal{O}|\Psi_0\rangle}{\mu}\ .$$

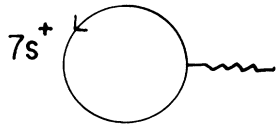

FIG. 1. Diagrammatic representation of the zero-order valence contribution to the hyperfine field.

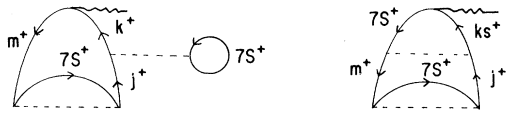

FIG. 3. Major (a) EPV and (b) consistency diagrams.

Terms in Eq. (5) involving specific values of the indices N and M are referred[6,11,21] to as (N,M) terms. Each term in the expansion can be expressed as a diagram through the use of rules given in earlier work.[21] The major diagrams we have evaluated in this work refer to[6,21] direct, exchange core-polarization (ECP), consistency, and correlation contributions to the hyperfine interaction and are shown in Figs. 1–5. The expressions that one has to evaluate for these diagrams involving the occupied and excited states have been given previously.[7,11]

The nuclear moment μ in the operator $\mathcal{O}$ in Eq. (6) is that of a point dipole located at the center of the nucleus. In reality the nuclear moment is distributed throughout the nuclear volume. This distribution of the nuclear moment could produce a significant reduction of the hyperfine field which must be taken into account. We have therefore reduced all our calculated results by 4% as an estimate of the effect of this spatial distribution of the nuclear moment. This figure was based on the results of Kopfermann,[22] who evaluated this effect for a number of atomic systems using a hydrogenic approximation for the electronic wave functions. This is expected to be quite satisfactory since one is interested in the region near and inside the nucleus. Adopting Kopfermann's prescription allows one to take account of the departure from volume uniformity of the nuclear magnetic moment distribution.

III. RESULTS AND DISCUSSION

The primary results of our calculation of the hyperfine field are presented in Table I, along with the experimentally measured value of the field. The latter is determined from the experimentally observed hyperfine constant[2] through division by the magnetic moment obtained[1] from Zeeman measurements. The valence contribution of 971 T in Table I refers to the zero-order contribution (Fig. 1) to the hyperfine field due to the unperturbed $7s$ valence electron. The second entry in Table I comes from the first-order [(0,1)] diagrams in Fig. 2. Figure 2(a) represents the ECP (Ref. 5, 6, 11, and 21) effect which results from the fact that only the up-spin core electrons experience an exchange interaction with the valence electron, leading to different spin densities at the nucleus for the up- and down-spin electrons in a given core state. Figure 2(b) is the phase-space[11,21] diagram which arises because, unlike the $7s^+$ state, the $7s^-$ state is unoccupied and is therefore available as a particle (excited) state for the perturbation of the down-spin core electrons. Figure 2(a) derives a contribution of 124 T from the core s states and -4 T from the p states, the latter being possible[5] only in relativistic theory. As in the case of other alkaline-earth-metal ions[23,24] and alkali-metal atoms,[7] the outermost core state, $6s$, is the major contributor to the ECP effect, because of its stronger exchange with the $7s^+$ electron and weaker binding compared to the other core s electrons. Figure 2(b) contributes 17 T arising from all the core s states, with $6s$ again being the major contributor. Since both the ECP and phase-space contributions are essentially one-electron effects they are grouped together.

On going to second order [(0,2) and (1,1)] in perturbation theory one obtains both correlation diagrams involving many-electron effects and several diagrams which

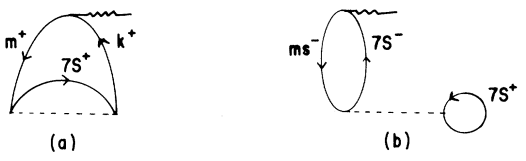

FIG. 2. Diagrams representing the (a) ECP and (b) phase-space contributions to the hyperfine field.

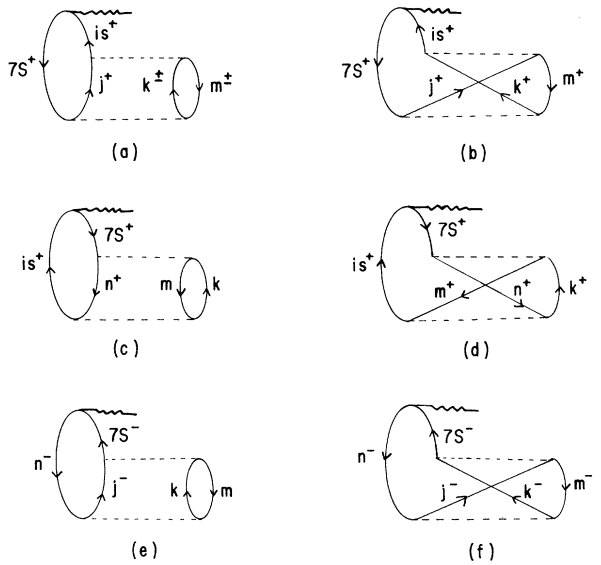

FIG. 4. The (0,2) correlation diagrams. (a) and (b) are the direct and exchange diagrams, respectively, with the second two-electron vertex connected to the particle line on the left bubble. (c) and (d) are the direct and exchange hole-line diagrams while (e) and (f) are the direct and exchange phase-space diagrams.

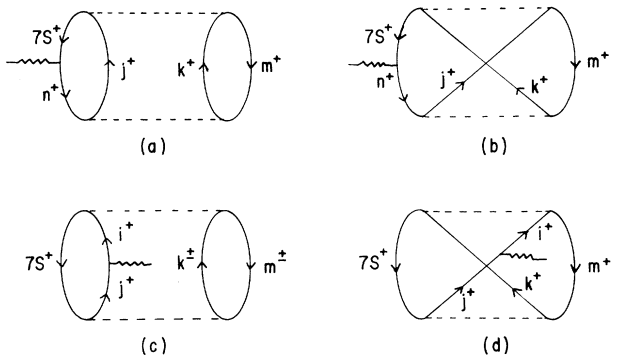

FIG. 5. (1,1)-type correlation diagrams. (a) and (b) are the direct and exchange hole-line diagrams while (c) and (d) are the direct and exchange particle-line diagrams.

represent corrections[7,21] to the one-electron diagrams of Fig. 2. Among the latter class are the exclusion principle violating (EPV) diagrams which arise as a correction because of our use of the V^{N-1} potential and the consistency diagrams which correct for the change in the potential experienced by the electrons because of the changes in the electron density produced by the ECP effect. Typical EPV and consistency diagrams are shown in Figs. 3(a) and 3(b), respectively. The EPV and consistency diagrams were found to contribute 4 T to the hyperfine field, as shown in Table I. The sum of the ECP, phase-space, EPV, and consistency diagrams, all representing one-electron interactions of the core electrons with the valence electron, is 141 T. This sum will henceforth be referred to as the net ECP contribution.

The ratio of the net ECP contribution to the valence contribution is seen from Table I to be about 15%, close to that for the Ba^+ ion,[23] the next heaviest of the alkaline-earth-metal ions, a trend similar to that found within the alkali-metal atom series.[7] This ratio of 15% in Ra^+ is also smaller than the corresponding ratio of 17% found in the neutral Fr system,[3] a trend similar to that found in going from[24] Mg^+ to Na and from[23] Ba^+ to Cs.

The fourth entry of 204 T in Table I gives the contribution of the (0,2)-type correlation diagrams shown in Fig. 4, while the fifth entry of -57 T is that for the (1,1)-type correlation diagrams of Fig. 5. These diagrams involve two simultaneously excited electrons and thus represent true many-body correlation effects.[21] We have evaluated these diagrams, with m in these diagrams indicating the $5d$, $6s$, and $6p$ core states (the other core states making negligible contributions), up to the $l=4$ multipole moment of the $1/r_{12}$ interaction. From earlier investigations,[11] it has been found that satisfactory convergence is attained when one uses multipole components of $1/r_{12}$ up to this order. Most of the correlation contribution comes from the $6p$ state while the $6s$ state gives the smallest contribution, as may be seen from Table II, where the contributions of the (0,2) and (1,1) diagrams from each m are given explicitly.

As in earlier investigations on other systems,[5–7,11,21] the major higher-order diagrams are expected to be those that are related to the major second-order correlation diagrams involving additional $1/r_{12}$ vertices. By studying a number of such third-order diagrams we have been able to estimate the effect of the higher-order contribution to be about -20 T, the sixth entry in Table I. The ratio of the net correlation contribution to the valence contribution is seen from Table I to be 13%, smaller than the corresponding ratio of 28% for the isoelectronic system francium. This is expected since the Ra^+ ion is positively charged, its states being less deformable with respect to the polarization effect associated with correlation. Also this same ratio for Ba^+ is 24%, which is larger than for Ra^+, in agreement with the trend in going from Cs to Fr, the physical reason for which has been discussed in earlier work.[7]

Our total hyperfine field is seen from Table I to be 1239 T, in excellent agreement with the experimental field of 1226(4) T. From a consideration of computational accuracy and the importance of higher-order correlation effects and higher multipole moments of $1/r_{12}$ beyond $l=4$, we expect our calculated hyperfine field to have an accuracy of about 2%, which is a conservative estimate. Using the experimentally determined coupling constant[2] of 22 920 MHz and our calculated hyperfine field we deduce a theoretical magnetic moment of $0.607(12)\mu_N$ for ^{213}Ra, in excellent agreement with the experimentally determined moment[1] of $0.6133(18)\mu_N$.

We shall next analyze the correlation contributions in more detail since such an analysis can provide valuable insight into the nature of the correlation effects. Tables III and IV present the contributions to the field from individual correlation diagrams involving the $6p$ and $5d$ shells, respectively. From Table III we see that the dominant diagrams are those of Fig. 4(a) and its exchange counterpart, Fig. 4(b). This is not surprising, since these have proved to be the dominant diagrams in other similar systems, namely, neutral alkali-metal atoms[7] and the alkaline-earth-metal ions.[23,24] The next largest contribution, of about a quarter of the (0,2) contribution and 4% of the net field, comes from the (1,1) diagrams of Figs. 5(a) and 5(b). This result is different from that in neutral alkali-metal atoms, where, for instance, in rubidium[7] it was found to be less than 0.2% of the total hyperfine

TABLE I. Contributions (in tesla) from various mechanisms to the hyperfine field of $^{213}Ra^+$. All contributions have been reduced by 4% to account for the spatial distribution of the nuclear magnetization.

Mechanism	Contribution (T)
Valence	971
ECP plus phase space	137
EPV plus consistency	4
(0,2) correlation	204
(1,1) correlation	−57
Third-order correlation[a]	−20
Total hyperfine field	1239
Experimental field[b]	1226(4)

[a]Estimated from major second-order correlation diagrams.
[b]Taken from Table II of Ref. 1.

TABLE II. Total contributions (in tesla) from the (0,2) and (1,1) diagrams to the correlation contributions from the $6p$, $5d$, and $6s$ states.

State	(0,2) contribution	(1,1) contribution	Total
$6p$	137	−38	99
$5d$	56	−18	38
$6s$	11	−1	10
Total	204	−57	147

field. This difference between the situation in Rb and Ra^+ could be a result of the fact that there are a number of (1,1) diagrams with comparable magnitude and different signs, the cancellation being less acute in Ra^+ than in Rb. The hole-line diagrams of Figs. 4(c) and 4(d) and the phase-space diagrams of Figs. 4(e) and 4(f) make the next most important contribution and are of comparable magnitude for the $6p$ diagrams. For the $5d$ case the phase-space diagrams are considerably larger, about 4.5% of the net field compared to 1.8% for $6p$. The (1,1) diagrams of Figs. 5(c) and 5(d) give negligible contributions.

The results in Tables III and IV also show the variation in the contribution to the correlation effect as a function of the multipole moment l of the electron-electron interaction. It is interesting that for the direct correlation diagrams in Figs. 4 and 5, it is the dipole correlation effect associated with $l=1$ that makes the major contribution. This dominance of the $l=1$ contribution over the $l=0$ contribution has been observed in other alkali-metal atoms[7] including Fr, which is isoelectronic with Ra^+. It may result from the fact that the $l=1$ contribution involves excitations to states with similar quantum numbers (such as $7s \Longrightarrow 7p$ and $6p \Longrightarrow 6d$) while the $l=0$ terms do not. The small energy denominators, coupled with the fairly large $1/r_{12}$ matrix elements, could lead to the observed dominance. The decrease in the correlation effect beyond $l=1$ can again be understood through the increase in the energy denominators and decrease in the two-electron interaction matrix elements as the states become less alike.

Another interesting feature in terms of the variation of the correlation contribution with the multiple moment is the slower decrease of the exchange contribution with increasing l as compared to the direct effect. This difference in behavior can be understood physically by comparing, for instance, the direct and exchange diagrams, Figs. 4(a) and 4(b), for the quadrupole ($l=2$) excitation. Thus, considering the vertices associated with the $1/r_{12}$ operator, the first of the diagrams contains the excitations $7s \Longrightarrow 6d$ and $6p \Longrightarrow 7p$ at the first vertex and $6d \Longrightarrow 8s$ and $6p \Longrightarrow 7p$ at the second while for Fig. 4(b), the corresponding excitations are $7s \Longrightarrow 6d$, and $6p \Longrightarrow 7p$ and $8s \Longrightarrow 7p$ and $6p \Longrightarrow 6d$. The first set of excitations is the same for both diagrams while the second involves pairs of states at the vertices involving $1/r_{12}$ which are more similar to each other in the case of the diagram, Fig. 4(b), than in Fig. 4(a) and therefore lead to larger matrix elements. The slower decrease of the exchange correlation effect as compared to the direct (which has sign opposite to that of the exchange) makes their sum decrease faster with l and makes the neglect of contributions beyond $l=4$ well justified, the influence of higher l being estimated to be no more than 5% of the net correlation contribution.

As to the last item of discussion, we would like to comment on the relationship of the results of the present calculation to some earlier evaluations[8−10] of the hyperfine field in the Ra^+ ion. One of these was an earlier investigation[8] by a number of the authors of the present paper using the RLCMBPT procedure. A second one[10] involved the evaluation of the ECP contribution through a differential equation (DE) technique[25,26] and the correlation contribution by a hybrid of the DE technique and the RLCMBPT procedure in which the effect of the electron-electron interaction ($1/r_{12}$) operator is handled

TABLE III. Contributions from various diagrams to the $6p$-shell correlation contribution in tesla to the hyperfine field at the nucleus of the $^{213}Ra^+$ ion.

	Diagrams[a]									
Multipole component	Fig. 4(a)	Fig. 4(b)	Fig. 4(c)	Fig. 4(d)	Fig. 4(e)	Fig. 4(f)	Fig. 5(a)	Fig. 5(b)	Fig. 5(c)	Fig. 5(d)
$l=0$	15	2	−7	2	−3	−2	−3	−1	4	2
$l=1$	106	1	−14		−26	1	−54	3		2
$l=2$	66	−25	−2	0	6	1	8	1		
$l=3$	29	−17			2	−1	3	−3		
$l=4$	8	−5			1	−1	1	−1		
Total	224	−44	−23	2	−20	−2	−45	−1	4	4

[a]All values have been reduced by 4% to account for the distribution of the nuclear moment.

TABLE IV. Contributions from various diagrams to the 5*d*-shell correlation contribution to tesla to the hyperfine field at the nucleus of the $^{213}Ra^{+}$ ion.

	Diagrams[a]									
Multipole component	Fig. 4(a)	Fig. 4(b)	Fig. 4(c)	Fig. 4(d)	Fig. 4(e)	Fig. 4(f)	Fig. 5(a)	Fig. 5(b)	Fig. 5(c)	Fig. 5(d)
$l=0$	18	0	−6	1	−6	0	−3	0	3	0
$l=1$	98	−5	−1	−1	−44	2	−19	1		0
$l=2$	8	0	−2		−6	0	−1	0		
$l=3$	7	−6			−6	6	0	1		
$l=4$	1	−1			0	−1	0	0		
Total	132	−12	−9	0	−62	7	−23	2	3	0

[a]All values have been reduced by 4% to account for the distribution of the nuclear moment.

as in the present work while that of the hyperfine vertex is treated by the DE procedure. A third calculation[9] utilized the DE technique[25,26] for the ECP effect and extrapolated the correlation contribution from the nonrelativistic results in lighter alkaline-earth-metal ions and alkali-metal atoms by the DE technique.[26] Lastly there is an evaluation of the hyperfine field available through the use of the semiempirical Goudsmit-Fermi-Segre formula.[12]

The primary difference between this investigation and the earlier one[8] by the present group is the incorporation of (1,1) correlation diagrams in the current work. This accounts for the difference in the magnetic moment of ^{213}Ra quoted in Ref. 1 using the hyperfine field from our earlier work[8] ($0.62\mu_N$) and the present value [$(0.607\pm0.012)\mu_N$].

Turning next to the other earlier calculations,[9,10] we consider first the results shown in the second line of Table V. The main difference between the procedure[10] used to obtain these results and the conventional RLCMBPT procedure[6] used in the present work is the handling of the ECP vertex using a DE technique[25,26] rather than a summation over the basis states. Comparing the results for the valence, ECP, correlation, and total contributions to the hyperfine field in the second line of Table V with ours in the first line, one finds good overall agreement between the two, especially in the net hyperfine field, the result in Ref. 10 being about 2.2% smaller than our result which is in essential agreement with experiment.[1] It is instructive to examine the small but significant differences in the individual contributions from the two calculations which are in some cases more pronounced than for the net hyperfine field, since such an analysis provides insights into the natures and relative accuracies of the two procedures. Thus, considering the valence contributions first, the result in the second line of Table V is about 14 T or 1.5% smaller than our result. In looking for sources to explain this difference, one can analyze first the treatment of the finite charge and magnetic moment distributions of the nucleus in the two calculations. Considering first the nuclear charge distribution, the work in Ref. 10 made use of a nonuniform radial charge distribution in contrast to the uniform distribution used in this work. However, the potentials that would be produced by the two distributions are very similar, with the potential in Ref. 10 slightly more attractive[27] inside the nuclear radius than that used in the present work. This feature of the potential would be expected to lead to a small increase in the second line for the valence contribution over the first rather than to the decrease that is observed. As regards the effect of the magnetic moment distributions, this could be a possible source of difference since we have used a nonuniform magnetic moment distribution in contrast to the uniform one used in Ref. 10. Another source

TABLE V. Comparison of the results from different theoretical investigations and experiment for the hyperfine fields (in tesla) and nuclear magnetic moments of ^{213}Ra.

Reference	Valence	ECP	Correlation	Total	μ_I/μ_N
This work	971	141	127[a]	1239	0.607(12)
10	957.0	158.3	150.7	1266.0	0.594(6)[b]
9	978	159.6[c]	166.4[d]	1304(65)[b]	0.58(3)[b]
1 (expt.)				1226(4)[b]	0.6133(18)[b]

[a]The result shown here refers to the net correlation contribution obtained by adding the higher-order contributions of −20 T to the net second-order contributions in Table II, as explained in the text.
[b]Taken from Table II of Ref. 1.
[c]Obtained by subtracting the valence contribution from the polarization contribution quoted in the second row of Table I of Ref. 8.
[d]Obtained by subtracting the valence and ECP contributions from the total field given in Table II of Ref. 1.

of difference, which we feel is the most likely one, is the calculation of the valence wave function in Ra^+ by the different procedures in Ref. 10 and the present work. In our work, as explained in Sec. II, we have used for the occupied core and valence states the Hartree-Fock orbitals for Ra^+. In Ref. 10, however, for the valence state, the Hartree-Fock 7*s* orbital for the Ra^{2+} ion has been employed. In the latter, the 7*s* is unoccupied and therefore the core states are expected to be less shielded than in Ra^+ and therefore more tightly bound. As a consequence of this, the core electrons would in turn shield the nucleus more strongly in Ra^{2+} than in Ra^+, causing the 7*s* valence orbital in Ra^{2+} to be less tightly bound and have a smaller density at the nucleus. This effect is in the right direction to explain the difference between the valence contribution in Ref. 10 and ours. The difference in the two potentials is also felt in the ECP contributions as discussed next.

The ECP contributions from the present calculation and that of Ref. 10 are seen from Table V to have the opposite trend to that of the valence contribution. The ECP contribution from Ref. 10 is seen to be larger by about 17.3 T or 12% as compared to that from the present work. In looking for an explanation of this difference there appear to be at least two possible sources. One possibility is that the difference in the ECP contributions arises from differences in the charge and moment distributions. This does not appear likely because it would have led to a difference in the same direction as for the valence contribution. The other possibility and again the one we consider most likely is connected with the different potentials used in Ref. 10 and our work for generating the core states. Thus, due to the reasons detailed in the preceding paragraph in comparing our valence contribution with that in Ref. 10, the core states in Ref. 10 are expected to be more tightly bound, leading to larger densities at the nuclei when exchange polarized by the valence electron. This would lead to an ECP contribution larger than ours as is observed in Table V. It is satisfying that a common origin has been found for the differences in the valence and ECP contributions which tend to neutralize each other substantially.

Regarding the correlation contribution, the result in Ref. 10 is 23.7 T, or about 19% higher than our result in Table V. The authors of Ref. 10 do not supply details on the contributions from individual diagrams as listed in the present work in Tables III and IV. We can therefore compare only the net correlation contributions. However, it is possible to infer the reasons for the difference in the net correlation contributions from an examination of the natures of the (0,2) and (1,1) correlation diagrams in Figs. 4 and 5. Thus, for the (0,2) correlation diagrams in Fig. 4, the hyperfine vertex involves the 7*s* valence and the excited *s* states in the system. As discussed earlier in comparing the valence and ECP contributions, the core states in Ref. 10 are expected to be more tightly bound than ours, leading to stronger screening of the nuclear charge and hence less tightly bound valence and excited states. One would therefore expect the (0,2) diagrams in Ref. 10 to have lesser contribution than ours. On the other hand, it is not clear that the (1,1) diagrams of the type in Figs. 5 can be included with the procedure used in Ref. 10. This is because in Figs. 5(a) and 5(b) the hyperfine vertex involves the perturbation effect on the valence 7*s* state with restricted excitations to only the phase space available from the other core *s* states because of their excitation to higher states through correlation interactions with other occupied states. It would be rather difficult to set up appropriate differential equations to handle this type of perturbation of the valence state due to the hyperfine interaction Hamiltonian. Secondly, the diagrams in Figs. 5(c) and 5(d) require perturbations of excited bound and continuum states, which, because of their relatively large number would be rather time-consuming to handle by the DE technique. The observation that the net correlation contribution in Ref. 10 is larger than ours indicates that the neglect of the negative contribution of the (1,1) diagrams in Ref. 10 counterbalances the somewhat weaker positive contribution from the (0,2) diagrams in Fig. 4.

The procedure for the results represented in the third line (Ref. 9) in principle involved the DE technique[26] in evaluating both the ECP and correlation contributions, although the correlation contribution in Ref. 9 for Ra^+ was actually estimated using the results for other systems as a base. The authors of this calculation make no mention of the effect of the magnetization distribution and do not seem to have taken it into account. Thus, although the valence contribution seems to agree well with our result, a 4% reduction would actually make their result even smaller than that on the second line corresponding, to Ref. 10. The ECP result agrees well with that of the second calculation, as one would expect, given the similarities of the techniques used, even after a 4% reduction is applied, and is again higher than our result as in the case of Ref. 10. The remarks made earlier concerning the difference between the result of the current work and that of the second calculation apply here as well. The correlation result is about 6% larger than that of Ref. 10 after the 4% reduction due to nuclear moment distribution is included, and about 26% larger than the contribution calculated in the current work. The difference between the results in Refs. 9 and 10 is most likely a consequence of the fact that the correlation contribution in Ref. 9 is actually an estimate. In view of this, one cannot attach too much significance to the somewhat better agreement one obtains with our results and experiment in Table V after a 4% correction due to the nuclear moment distribution is applied to the net hyperfine field in Ref. 9 (Table V) than was the case for Ref. 10.

Finally, we would like to comment on the very good agreement found[2] between the magnetic moment of ^{213}Ra obtained using the Goudsmit-Fermi-Segre formula[12] to derive the hyperfine field at the nucleus and the experimental value from the Zeeman measurement[1] as well as the theoretical value in the present work. This agreement is remarkable,[1] considering the fact that, from Table V, the combination of ECP and correlation contributions is sizable, about 30% of the direct contribution. This feature also appears to apply in general to the alkali-metal atoms as well, as may be seen from Ref. 12 (p. 136), where the predicted magnetic moments from the ob-

served hyperfine constants combined with hyperfine fields obtained from the Goudsmit-Fermi-Segre formula are seen to be in reasonably good agreement with directly measured nuclear magnetic moments by methods such as nuclear magnetic resonance. A possible reason for this success of the Goudsmit-Fermi-Segre formula[12] could be that it utilizes the effective quantum number $n_s = n - \sigma$, where n is the principal quantum number and σ is the quantum defect obtained from the experimental ionization energy in the valence state. The factor $1 - d\sigma/dn$ is also derived from experimental ionization energies for valence and excited states. Since the experimental ionization energies include electron-electron interaction effects, these effects could get included indirectly in the Goudsmit-Fermi-Segre expression[12] for the spin density. It would be useful, although rather complicated, to trace in more detail the origins in both RLCMBPT and configuration-interaction procedures, for this remarkable agreement.

IV. CONCLUSION

In conclusion, essentially complete agreement has been achieved between the RLCMBPT calculation in the present work and the Zeeman measurement of the nuclear moment of the ^{213}Ra nucleus. A detailed breakdown of the contributions to the hyperfine field from various mechanisms is presented to provide insights into the relative importance of the different factors which influence the hyperfine field. Our result for the hyperfine field also agrees quite well with the results of calculations[9,10] using the DE approach for either only[10] the hyperfine vertex or both[9] the hyperfine vertex and the electron-electron interaction vertices. However, there are small but significant differences in the individual contributions to the hyperfine field from the present work and from earlier investigations which have been analyzed here and possible sources for these differences have been suggested. It is hoped that this analysis will stimulate future investigators to carry out similar comparisons as here between the results using different many-body procedures, which would ultimately lead to better insights into the natures of all the different procedures being currently used[6,9,10,14] in relativistic many-body theory for atomic systems. We would like to conclude by reiterating that there is significant cancellation among the differences between Ref. 10 and the present work in the contributions from different mechanisms to the hyperfine field. This is to be expected since many-body perturbation-theoretical calculations using different zero-order Hamiltonians, when carried out to convergence, should, in principle, lead to identical results.

*Present address: GTE Electrical Products, 100 Endicott Street, Danvers, MA 01923.

[1]E. Arnold, W. Borchers, M. Carre, H. J. Doung, P. Juncar, J. Lerne, S. Lieberman, W. Neu, R. Neugart, E. W. Otten, M. Pellarin, J. Pincard, G. Ulm, J. L. Vialli, and K. Wendt, Phys. Rev. Lett. **59**, 771 (1987).

[2]S. Ahmad, W. Klempt, R. Neugart, E. W. Otten, K. Wendt, and C. Ekstrom, Phys. Lett. **133B**, 47 (1983); K. Wendt, S. A. Ahmad, W. Klempt, R. Neugart, E. W. Otten, and H. H. Stroke, Z. Phys. D **4**, 227 (1987).

[3]Mina Vajed-Samii, J. Andriessen, B. P. Das, S. N. Ray, T. Lee, and T. P. Das, Phys. Rev. Lett. **48**, 1330 (1982); **49**, 1466 (1982); **49**, 1800 (1982).

[4]V. A. Dzuba, V. V. Flambaum, and O. P. Sushkov, J. Phys. B **17**, 1953 (1984).

[5]J. Andriessen, K. Raghunathan, S. N. Ray, and T. P. Das, Phys. Rev. B **15**, 2533 (1977); J. Andriessen and D. van Ormondt, J. Phys. B **8**, 1993 (1975).

[6]J. Andriessen, D. van Ormondt, S. N. Ray, and T. P. Das, J. Phys. B **11**, 2601 (1978).

[7]Mina Vajed-Samii, S. N. Ray, and T. P. Das, Phys. Rev. A **20**, 1787 (1979); Mina Vajed-Samii, J. Andriessen, B. P. Das, S. N. Ray, T. Lee, and T. P. Das, J. Phys. B **15**, L379 (1982).

[8]R. Neugart, E. W. Otten, K. Wendt, S. Ahmad, Surya N. Panigrahy, R. W. Dougherty, K. C. Mishra, T. P. Das, and J. Andriessen (unpublished work), quoted in Ref. 1.

[9]J. L. Heully and A. M. Martensson-Pendril, Phys. Scr. **31**, 169 (1985).

[10]V. A. Dzuba, V. V. Flambaum, and O. P. Sushkov, Phys. Scr. **32**, 507 (1985).

[11]S. N. Panigrahy, R. W. Dougherty, T. P. Das, and J. Andriessen, Phys. Rev. A **40**, 1765 (1989).

[12]H. Kopfermann, *Nuclear Moments* (Academic, New York, 1958), p. 123.

[13]B. P. Das, J. Andriessen, Mina Vajed-Samii, S. N. Ray, and T. P. Das, Phys. Rev. Lett. **49**, 32 (1982).

[14]W. R. Johnson, M. Indrees, and J. Sapirstein, Phys. Rev. A **35**, 3218 (1987).

[15]J. Sapirstein, Phys. Scr. **36**, 801 (1987); W. R. Johnson, S. A. Blundell, and J. Sapirstein, Phys. Rev. A **37**, 2764 (1988); **38**, 2699 (1988).

[16]P. G. H. Sandars, J. Phys. (Paris) Colloq. **31**, C4-225 (1970).

[17]K. Raghunathan, S. N. Ray, J. Andriessen, and T. P. Das, Phys. Rev. Lett. **44**, 312 (1980).

[18]T. P. Das, *Relativistic Quantum Mechanics of Electrons* (Harper & Row, New York, 1973), Chap. 7.

[19]A. H. Stroud and Don Secrest, *Gaussian Quadrature Formulas* (Prentice-Hall, Englewood Cliffs, NJ, 1966).

[20]K. A. Brueckner, Phys. Rev. **100**, 36 (1956); J. Goldstone, Proc. R. Soc. London, Ser. A **239**, 267 (1957).

[21]Edward S. Chang, Robert T. Pu, and T. P. Das, Phys. Rev. **174**, 1 (1968).

[22]H. Kopfermann, *Nuclear Moments* (Ref. 12), p. 382.

[23]S. Ahmad, J. Andriessen, K. Raghunathan, and T. P. Das, Phys. Rev. A **25**, 2923 (1982).

[24]S. Ahmad, J. Andriessen, and T. P. Das, Phys. Rev. A **27**, 2790 (1983).

[25]R. M. Sternheimer, Phys. Rev. **86**, 316 (1952); G. D. Gaspari, Wei-Mei Shyu, and T. P. Das, *ibid.* **134**, A852 (1964).

[26]S. Garpman, I. Lindgren, J. Lindgren, and J. Morrison, Z. Phys. A **276**, 167 (1976).

[27]S. N. Panigrahy, Ph.D. thesis, State University of New York at Albany, Albany, New York, 1990.